Available online at www.sciencedirect.com
ScienceDirect
Chinese Journal of Natural Medicines 2020, **18**(2): 148–160
doi: 10.1016/S1875-5364(20)30015-7
Chinese Journal of Natural Medicines

Comprehensive analysis of the chemical constituents in sulfur-fumigated Lonicerae Japonicae Flos using UHPLC-LTQ-Orbitrap mass spectrometry

LIU Zi-Han[1], WANG Yu-Qi[1], MEI Xiao-Dan[1], WANG Fei[1], YANG Xian-Zhao[2], LI Xiao-Dong[3], JIANG Feng[2, *], ZHANG Jia-Yu[4, *]

[1] *School of Chinese Pharmacy, Beijing University of Chinese Medicine, Beijing 102488, China;*
[2] *BUCM Institute of Liver Diseases, Dongzhimen Hospital affiliated to Beijing University of Chinese Medicine, Beijing 100700, China;*
[3] *Department of Hepatology, Hubei Provincial Hospital of Traditional Chinese Medicine, Wuhan 430061, China;*
[4] *School of Pharmacy, Binzhou Medical University, Yantai 264003, China*

Available online 20 Feb., 2020

[ABSTRACT] Lonicerae Japonicae Flos (LJF), a kind of traditional Chinese medicines (TCMs), has functions of detoxifying and evacuating heat. In the study, a method based on ultra-high performance liquid chromatography coupled with linear ion trap-Orbitrap mass spectrometry (UHPLC-LTQ-Orbitrap MS) was developed for the chemical constituent analysis of organic acids, flavonoids, iridoids and new-generated compounds in sulfur-fumigated LJF (SF-LJF). Based on the accurate mass measurement (< ± 5 ppm), chromatographic behavior and diagnostic product ions (DPIs), 113 constituents were unambiguously or tentatively characterized from SF-LJF extract, including 46 chlorogenic acids, 19 flavonoids, 29 iridoid glycosides and 19 newly-generated compounds (including 17 sulfur-containing derivatives). In addition, 5-CQA (5-caffeoylquinic acid, chlorogenic acid) was chosen to be sulfur-fumigated for the result validation. It was found that the most significant change of LJF after sulfur fumigation was the occurrence of sulfate or sulfite esterification reactions, which resulted in the emergence of many new sulfur-containing components. Our results demonstrated that the established method was a useful and efficient analytical tool to comprehensively characterize the material basis of SF-LJF, and also an excellent guidance of quality control about LJF.

[KEY WORDS] Sulfur fumigation; Lonicerae Japonicae Flos; Chemical components analysis; UHPLC-LTQ-Orbitrap MS
[CLC Number] R917 **[Document code]** A **[Article ID]** 2095-6975(2020)02-0148-13

Introduction

Lonicerae Japonicae Flos (LJF, also named as *Jinyinhua* in Chinese) originates from the dried buds or blooming flowers of *Lonicera japonica* Thunb. [1]. As a kind of famous traditional Chinese medicine (TCM), LJF is mainly distributed in China, Japan and Southeast Asia. It has been widely used as TCM owing to its various pharmacological effects such as anti-inflammatory, anti-allergic, anti-virus, anti-oxidation, which was also commonly known as "antibiotics in TCMs" [2-4]. Additionally, LJF containing organic acids, flavonoids, iridoids and volatile oils has been universally employed to treat carbuncle, throat arthralgia, erysipelas, heat toxin, hemorrhagic dysentery, wind-heat cold, febrile fever and the other symptoms for several thousands of years [5-7]. In a word, LJF is proverbially applied in food, cosmetics, spices and ornamental plants, and so on.

The traditional processing methods of LJF are sun or shade drying, while the modern methods have spring up including steam drying, hot air drying, hot air-microwave combination drying and sulfur fumigation, *etc*. Among them, sulfur fumigation has been applied to pretreat LJF during post-harvest handling stage in order to preserve color and fresh-

[Received on] 09-Sep.-2019
[Research funding] This work was supported by Beijing Nova Program (No. Z171100001117029), Beijing University of Chinese Medicine Fund for Distinguished Young Scholars (No. 2018-JYB-XJ008), the Independent Topic Selection of Beijing University of Chinese Medicine (Innovation and Entre-preneurship Project, No. 2019-JYB-XSCXCY-06), and the Second Batch of Scientific Research Projects for the Construction of National TCM Clinical Research Base (JDZX2015181).
[*] **Corresponding author]** E-mail: jiangfeng@bucm.edu.cn (JIANG Feng); E-mail: zhangjiayu0615@163.com (ZHANG Jia-Yu)
These authors have no conflict of interest to declare.

ness, keep moist and prevent moulds and insects [8]. Although sulfur fumigation has been also applied to many other TCMs, such as Dioscoreae Rhizome (Shan-Yao), Angelicae Dahuricae Radix (Bai-Zhi) and Chrysanthemi Flos (Ju-Hua), the quality problems including chemical transformation, heavy metal and sulfur-dioxide residues brought from sulfur fumigation have frequently occurred, which may cause serious harm to human liver, kidney and the other organs [9-10]. Although sulfur fumigation has been officially restricted in China since 2005 [11], some illicit herbal farmers and wholesalers still misuse it during the post-harvest handling and storage of LJF. To our best knowledgement, the comprehensive chemical transformations in SF-LJF have not been available until now.

As more and more attentions have been paid to the food and drug safety, various satisfactory analytical methods have been developed in last two decades. Recently, ultra-high performance liquid chromatography coupled with high-resolution mass spectrometry (UHPLC-HRMS) has bloomed into a powerful approach for the rapid identification of constituents in TCMs. LTQ-Orbitrap analytical platform, which could offer multi-stage ESI-MS^n mass spectra using data-dependent analysis and accurate mass measurements within mass error of 5 ppm, benefits the analysis of small molecules in TCMs [12-15]. Meanwhile, a full scan mass spectrum acquired with a mass resolution of 30 000 (FWHM, calculated for *m*/*z* 200) for Orbitrap only needs 0.4 s, and provides no less than 25 data points across a peak of width at baseline of 10 s. Based on the above superiorities, UHPLC-LTQ-Orbitrap MS can provide reliable and effective technical support for TCMs component analysis.

In this study, we firstly established the laboratory simulation method to obtain SF-LJF samples, and then developed an UHPLC-LTQ-Orbitrap MS-based analytical method to comprehensively profile the chemical constituents in non-sulfur-fumigated LJF (NSF-LJF) and SF-LJF (Fig. 1).

Materials and Methods

Chemicals and reagents

NSF-LJF sample (specification: 500 g/bag, batch number: 20170526) was purchased from co-operative farmers in authenticated region named Pingyi city, Shandong province in China. The identity of NSF-LJF sample was authenticated to be the dried buds or blooming flowers of *Lonicera japonica* Thunb. by histological and morphological methods according to monograph of Chinese Pharmacopoeia (version 2015) by Prof. ZHANG Yuan in Beijing University of Traditional Chinese Medicine. The voucher specimen of NSF-LJF was deposited in School of Chinese Pharmacy, Beijing University of Chinese Medicine, Beijing city, China. Acetonitrile, methanol and formic acid of LC-MS grade were all purchased from Thermo Fisher Scientific (Fair Lawn, NJ, USA). All the other chemicals of analytical grade were provided by Beijing Chemical Works (Beijing, China). Deionized water used throughout the experiment was purified by Milli-Q Gradient Å 10 System (Millipore, Billerica, MA, USA). Grace Pure™ SPE C_{18}-Low solid-phase extraction cartridges (200 mg/3 mL, 59 μm, 70 Å) were purchased from Grace Davison Discovery Science (Deerfield, IL, USA).

(A) (B)

Fig. 1 The samples of Lonicerae Japonicae Flos (LJF, A) and sulfur-fumigated Lonicerae Japonicae Flos (SF-LJF, B)

Sixteen reference substances including seven organic acids, *i.e.* caffeic acid, chlorogenic acid (5-caffeoylquinic acid, 5-CQA), neochlorogenic acid (3-caffeoylquinic acid, 3-CQA), cryptochlorogenic acid (4-caffeoylquinic acid, 4-CQA), isochlorogenic acid A (3, 5-dicaffeoylquinic acid, 3, 5-CQA), isochlorogenic acid B (3, 4-dicaffeoylquinic acid, 3, 4-CQA) and isochlorogenic acid C (4, 5-dicaffeoylquinic acid, 4, 5-CQA); six flavonoids, *i.e.* chrysoeriol-7-*O*-neohesperidin, hyperoside, lonicerin, rutin, luteolin-7-*O*-*β*-D-glucoside and tricin-7-*O*-*β*-D-glucopyranoside; three iridoid glycosides, *i.e.* sweroside, secologanoside and secoxyloganin were purchased from Chengdu Must Biotechnology Co., Ltd. (Sichuan, China). All of their purities were determined to be no less than 98% by HPLC-DAD normalization of the chromatographic peak areas.

Preparation of SF-LJF and SF-5-CQA using laboratory simulation method

The obtained NSF-LJF sample was evaluated using acid distillation-iodimetric titration method according to Chinese Pharmacopoeia (version 2015). SF-LJF samples were prepared in laboratory following the modified procedures similar to that performed by illicit wholesalers [16]: LJF powders (200 g) were wetted with 20 mL water, and then put to stand for 0.5 h. Sulfur powders (20 g) were heated until it burned, and then the burning sulfur and wetted LJF powders were respectively put into the lower and upper layer of a desiccator. The desiccator was kept closed for 12 h. The SF-LJF samples were dried in a ventilated drying oven at 40 ºC for 12 h. In order to eliminate the differences generated from sample sampling, the SF procedure was carried out three times in parallel, and then the equivalent samples were mixed finally.

The preparation method of SF-5-CQA: 5-CQA reference substances (0.5, 1.0, 2.0, 2.5 and 5 mg) were respectively weighed, and each sample was then thoroughly mixed with 5.0 mg dextrin. Then SF-5-CQA was prepared according to the abovementioned preparation method.

Preparation of SF and NSF-LJF extract

The NSF-LJF (50 g) was extracted three times with 500 mL water under reflux for 2 h each. The combined solvent

was evaporated under reduced pressure to obtain 100 mL solution. Adequate ethanol was added in the mixture until the ethanol concentration reached up to 75%. And then, the mixture was stored under 4 ºC for 24 h. Finally, the solution was filtered and concentrated into the volume of 10 mL. Furthermore, the preparation method for SF-LJF extract was carried out using the same method mentioned above.

Solution preparation

Standard solution: Each reference standard was accurately weighed, dissolved in methanol to produce the standard solutions, which were stored in the refrigerator at 4 ºC prior to analysis. The mixed standard solution was diluted into a suitable working solution before it was used.

Sample solution: NSF-LJF (1 mL) and SF-LJF samples (1 mL) were respectively added into SPE cartridges which were orderly pretreated with methanol (5 mL) and deionized water (5 mL). And then, the SPE cartridges were successively washed with deionized water (5 mL) and methanol (3 mL). The methanol eluates were collected and then centrifuged at 14 000 r·min^{-1} for 15 min, respectively. The supernatants were used for the successive LC-MS analysis.

The solution of SF-5-CQA: The proper amount of SF-5-CQA reference substance was weighed and then its solution was made in the same way as above.

LC-MS conditions

The chromatographic analysis was performed on an Ultimate 3000 UHPLC system (Thermo Fisher Scientific, MA, USA), which was equipped with a binary pump, an autosampler, and a column compartment. The chromatographic separation was carried out using Waters ACQUITY UPLC HSS T3 C_{18} column (2.1 mm × 100 mm, 1.8 μm; Waters Corporation, Milford, MA, USA) at 40 ºC. Acetonitrile (solvent B) and 0.5% formic acid (FA) aqueous solution (solvent A) were used as the mobile phases. The flow rate was set to 0.30 mL·min^{-1} with a linear gradient as follows: 0−2 min, 5%−8% B; 2−7 min, 8%−10% B; 7−12 min, 10%−12% B; 12−15 min, 12%−16% B; 15−24 min, 16%−25% B; 24−26 min, 25%−95% B; 26−29 min, 95% B; 29−30 min, 95%−5% B; 30−33 min, 5% B. The injection volume was 5 μL.

HRMS spectral analysis was executed on an LTQ-Orbitrap *Velos* Pro mass spectrometer (Thermo Fisher Scientific, MA, USA) equipped with an electrospray ion (ESI) source. The optimized operating parameters in negative ion mode were set as follows: sheath gas flow rate of 30 arb, auxiliary gas flow rate of 10 arb, capillary voltage of −35 V, electrospray voltage of 3.0 kV, tube lens voltage of −110 V and capillary temperature of 300 ºC. The constituents were detected using full-scan MS analysis from *m/z* 100−1500 at a resolving power of 30 000. Data-dependent ESI-MS^2 analyses were triggered by the top three abundant ions while ESI-MS^3 analyses of the most-abundant product ions were followed. The collision energy for CID which was performed in LTQ with an activation of 0.25q and activation time of 30 ms was set to 40%. The isolation width was 2 amu, and the normalized collision energy was set to 35%. The dynamic exclusion (DE) was used to prevent duplication. The repeat count was set at 5 and the dynamic repeat time was 30 s with the dynamic exclusion duration at 60 s.

Data processing

Thermo Xcalibur 2.1 workstation (Thermo Fisher Scientific, MA, USA) was used for data acquisition and processing. In order to acquire as many fragment ions as possible, we targeted the peaks with intensity over 10 000 in negative ion mode for structural identification. Based on the accurate measurement, potential element compositions and occurrence of possible reactions, the predicted atoms for chemical formulas of all the deprotonated molecular ions were set as follows: C [0−50], H [0−100], O [0−30], S [0−2], N [0−3] and Ring Double Bond (RDB) equivalent value [0−15]. The maximum mass errors between the measured and calculated values were fixed within 5 ppm. All the relevant data including peak number, retention time, accurate mass, predicted chemical formula and corresponding mass error were recorded.

Results and Discussion

A sensitive and validated method based on UHPLC-LTQ- Orbitrap MS was developed for the comprehensive analysis of chemical constituents in SF-LJF (Fig. 2). The total ion chromatograms (TICs) of NSF-LJF and SF-LJF were obtained in negative ion mode (Fig. 3). According to the chromatographic retention behaviors, accurate mass measurements, mass fragmentation patterns and previous relevant literatures, 113 chemical constituents were positively and tentatively characterized from SF-LJF extract, including 46 chlorogenic acids (CGAs), 19 flavonoids, 29 iridoid glycosides and 19 newly-generated compounds (including 17 sul-

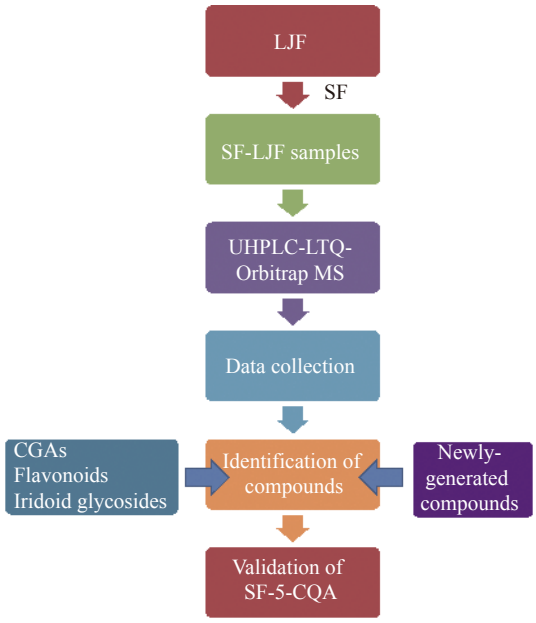

Fig. 2 The summary diagram of analytical strategy for identification of chemical constituents in SF-LJF

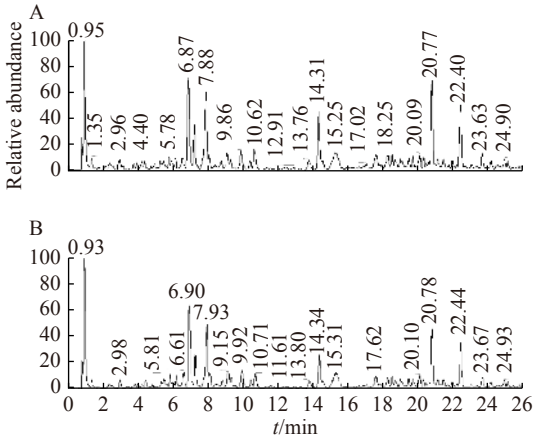

Fig. 3 The TIC chromatograms of SF-LJF (A) and NSF-LJF (B) in negative ion mode

fur-containing derivatives). Among them, 16 constituents were unambiguously identified (Table 1).

Structural identification of CGAs in SF-LJF extract

We have previously summarized the DPIs for CGAs on the basis of high-resolution and low-resolution MS data acquired. For example, DPIs for CQAs were determined to be the characteristic ions at *m/z* 191 [quinic acid − H]$^-$, 179 [caffeic acid − H]$^-$ and 173 [quinic acid − H − H_2O]$^-$. Meanwhile, the fragment ions at *m/z* 677 [TriCQA − H]$^-$, 515 [DiCQAs − H]$^-$ and 353 [CQA − H]$^-$ were also determined as the additional DPIs. As CGAs could be regarded as a series of esters which are formed by quinic acid and one or more certain cinnamic acids, the fragmentation pathways of the other CGAs such as *p*CoQA, FQA, and SQA should possess the similar mass fragmentation pathways with those of CQAs. Therefore,

Table 1 Identification of chemical constituents in SF-LJF using UPLC-LTQ-Orbitrap MS

Peak	t_R/min	Formula [M − H]$^-$	Theoretical mass *m/z*	Experimental mass *m/z*	Error (ppm)	MS/MS Fragment ions	Identification/Reactions
A1	6.18	$C_{16}H_{17}O_8$	337.0918	337.0926	–0.59	163 (100), 191 (9), 173 (5)	3-*p*CoQA
A2	10.42	$C_{16}H_{17}O_8$	337.0918	337.0926	–0.59	191 (100), 163 (6)	5-*p*CoQA
A3	10.93	$C_{16}H_{17}O_8$	337.0918	337.0924	–1.19	173 (100), 191(68), 163(10)	4-*p*CoQA
A4#	4.45	$C_{16}H_{17}O_9$	353.0867	353.0864	–0.96	191(100), 179 (52), 135 (9)	3-CQA
A5#	6.95	$C_{16}H_{17}O_9$	353.0867	353.0865	–0.44	191 (100), 179 (4), 135 (1)	5-CQA
A6#	7.77	$C_{16}H_{17}O_9$	353.0867	353.0872	1.53	173 (100), 179 (61), 191(17)	4-CQA
A7	7.71	$C_{17}H_{19}O_9$	367.1024	367.1021	–0.71	193 (100), 173 (8)	3-FQA
A8	12.94	$C_{17}H_{19}O_9$	367.1024	367.1021	–0.71	191 (100), 193 (5)	5-FQA
A9	13.28	$C_{17}H_{19}O_9$	367.1024	367.1022	–0.54	173 (100), 191 (21)	4-FQA
A10	5.84	$C_{18}H_{21}O_{10}$	397.1129	397.1128	–0.28	191 (100), 173 (14)	3-SQA
A11	6.63	$C_{18}H_{21}O_{10}$	397.1129	397.1127	–0.58	223 (100), 173 (19)	5-SQA
A12	17.69	$C_{25}H_{23}O_{11}$	499.1235	499.1232	–0.66	353 (100), 335 (27), 337 (28)	5-*p*Co-4-CQA
A13	18.88	$C_{25}H_{23}O_{11}$	499.1235	499.1233	–0.48	353 (100), 337 (8)	1-*p*Co-4-CQA
A14	22.61	$C_{25}H_{23}O_{11}$	499.1235	499.1231	–0.72	337 (100), 173 (2)	4-*p*Co-1-CQA
A15	23.00	$C_{25}H_{23}O_{11}$	499.1235	499.1233	–0.48	337 (100), 173 (6)	4-*p*Co-1-CQA
A16	23.21	$C_{25}H_{23}O_{11}$	499.1235	499.1234	–0.12	353 (100), 337 (25)	5-*p*Co-3-CQA
A17	23.46	$C_{25}H_{23}O_{11}$	499.1235	499.1233	–0.48	353 (100), 337 (17)	5-*p*Co-3-CQA
A18	24.89	$C_{25}H_{23}O_{11}$	499.1235	499.1233	–0.48	337 (100), 335 (7)	3-*p*Co-5-CQA
A19	25.15	$C_{25}H_{23}O_{11}$	499.1235	499.1230	–1.02	353 (100), 337 (17), 337 (9)	3-*p*Co-4-CQA
A20#	20.30	$C_{25}H_{23}O_{12}$	515.1184	515.1176	–1.53	353 (100), 335 (9)	3, 4-DiCQA
A21#	20.80	$C_{25}H_{23}O_{12}$	515.1184	515.1177	–1.28	353 (100), 434 (5)	3, 5-DiCQA
A22#	22.39	$C_{25}H_{23}O_{12}$	515.1184	515.1180	–0.82	353 (100), 173 (5)	4, 5-DiCQA
A23	3.26	$C_{22}H_{27}O_{14}$	515.1395	515.1387	–1.49	353 (100), 191 (25), 179 (20)	1/5-CQA glycoside
A24	4.23	$C_{22}H_{27}O_{14}$	515.1395	515.1392	–0.54	353 (100), 191 (75), 323 (6)	1/5-CQA glycoside
A25	5.26	$C_{22}H_{27}O_{14}$	515.1395	515.1391	–0.78	353 (100), 341 (35), 455 (29)	3-CQA glycoside

Continued

Peak	t_R/min	Formula $[M-H]^-$	Theoretical mass *m/z*	Experimental mass *m/z*	Error (ppm)	MS/MS Fragment ions	Identification/Reactions
A26	5.92	$C_{22}H_{27}O_{14}$	515.1395	515.1394	–0.19	353 (100), 323 (28), 191 (25)	4-CQA glycoside
A27	7.06	$C_{22}H_{27}O_{14}$	515.1395	515.1391	–0.78	353 (100), 191 (84), 395 (23)	3-CQA glycoside
A28	7.45	$C_{22}H_{27}O_{14}$	515.1395	515.1391	–0.78	323 (100), 191 (32), 353 (24)	4-CQA glycoside
A29	23.78	$C_{26}H_{25}O_{12}$	529.1341	529.1337	–0.81	367 (100), 173 (35), 335 (18)	3-C-4-FQA
A30	24.55	$C_{26}H_{25}O_{12}$	529.1341	529.1333	–1.51	367 (100), 349 (4)	5-C-3-FQA
A31	25.81	$C_{26}H_{25}O_{12}$	529.1341	529.1332	–1.63	367 (100), 179 (9)	*cis*-5-C-3-FQA
A32	5.40	$C_{23}H_{29}O_{14}$	529.1552	529.1542	–1.81	367 (100), 485 (82), 191 (69)	4-FQA glycoside
A33	6.65	$C_{23}H_{29}O_{14}$	529.1552	529.1542	–1.81	367 (100), 191 (66), 409 (13)	1/5-FQA glycoside
A34	14.85	$C_{23}H_{29}O_{14}$	529.1552	529.1545	–1.36	367 (100), 337 (51)	4-FQA glycoside
A35	15.36	$C_{23}H_{29}O_{14}$	529.1552	529.1545	–1.36	367 (100)	4-FQA glycoside
A36	19.22	$C_{23}H_{29}O_{14}$	529.1552	529.1545	–1.36	367 (100), 191 (51)	1/5-FQA glycoside
A37	16.67	$C_{31}H_{33}O_{17}$	677.1712	677.1716	0.63	515 (100), (75), 225 (20)	DiCQA-glycoside
A38	18.04	$C_{31}H_{33}O_{17}$	677.1712	677.1693	–2.79	515 (100), 353 (64), 335 (60)	DiCQA-glycoside
A39	26.55	$C_{34}H_{29}O_{15}$	677.1501	677.1484	–2.54	515 (100), 353 (6)	*cis*-1, 3, 5-TriCQA
A40	4.49	$C_9H_7O_4$	179.0339	179.0344	2.76	135 (100), 161 (7)	caffeic acid isomer
A41[#]	7.77	$C_9H_7O_4$	179.0339	179.0435	3.71	135 (100), 161 (2)	caffeic acid
A42	3.72	$C_7H_5O_4$	153.0182	153.0191	3.45	109 (100)	PCA isomer
A43	6.22	$C_7H_5O_4$	153.0182	153.0191	3.45	109 (100), 125 (3)	PCA isomer
A44	7.80	$C_7H_5O_4$	153.0182	153.0193	3.69	135 (100), 109 (77), 125 (2)	PCA isomer
A45	8.27	$C_9H_7O_2$	147.0441	147.0454	4.20	103 (100), 129 (41), 119 (12)	cinnamic acid isomer
A46	14.32	$C_9H_7O_2$	147.0441	147.0449	4.46	129 (100), 119 (60), 103 (48)	cinnamic acid isomer
B1[#]	19.00	$C_{21}H_{19}O_{11}$	447.0921	447.0900	–4.89	285 (100), 327 (3), 401 (1), 285 (1)	luteolin-7-*O*-glucoside
B2	21.00	$C_{21}H_{19}O_{11}$	447.0921	447.0901	–4.62	285 (100), 284 (78), 327 (15), 255 (8)	luteolin-7-*O*-glucoside isomer
B3	18.80	$C_{27}H_{29}O_{15}$	593.1501	593.1472	–4.85	285 (100), 269 (2), 447 (1), 327 (1)	lonicerin isomer
B4	19.71	$C_{27}H_{29}O_{15}$	593.1501	593.1467	–3.67	285 (100), 447 (67), 284 (22), 327 (9), 429 (5)	lonicerin isomer
B5[#]	20.50	$C_{27}H_{29}O_{15}$	593.1501	593.1471	–3.06	285 (100), 284 (7), 257 (4), 327 (3)	lonicerin
B6[#]	22.78	$C_{23}H_{23}O_{12}$	491.1184	491.1170	–1.40	476 (100), 329 (46), 328 (8), 314 (6)	tricin-7-*O*-D-glucopyranoside
B7	18.19	$C_{21}H_{19}O_{12}$	463.0871	463.0842	–3.95	301 (100), 342 (6), 300 (3), 445 (1)	hyperoside isomer
B8[#]	18.72	$C_{21}H_{19}O_{12}$	463.0871	463.0841	–3.52	301 (100), 300 (29), 343 (3), 179 (2)	hyperoside
B9	16.67	$C_{27}H_{29}O_{16}$	609.1450	609.1436	–2.39	285 (100), 447 (3), 301 (1)	rutin isomer
B10	17.84	$C_{27}H_{29}O_{16}$	609.1450	609.1429	–3.40	301 (100), 300 (64), 271 (10)	rutin isomer
B11[#]	18.29	$C_{27}H_{29}O_{16}$	609.1450	609.1408	–3.99	301 (100), 300 (40), 342 (8), 271 (6), 255 (4)	rutin
B12[#]	22.67	$C_{28}H_{31}O_{15}$	607.1657	607.1632	–4.27	299 (100), 284 (28), 443 (5), 285 (4), 487 (3)	chrysoeriol-7-*O*-*β*-D-neohesperidoside

Continued

Peak	t_R/min	Formula $[M-H]^-$	Theoretical mass *m*/*z*	Experimental mass *m*/*z*	Error (ppm)	MS/MS Fragment ions	Identification/Reactions
B13	20.61	$C_{22}H_{21}O_{11}$	461.1078	461.1066	–2.68	299 (100), 432 (86), 280 (81), 270 (51), 227 (42)	chrysoeriol-7-*O*-*β*-D-glucopyranosyl isomer
B14	22.51	$C_{22}H_{21}O_{11}$	461.1078	461.1064	–3.16	299 (100), 446 (96), 284 (7), 341 (5)	chrysoeriol-7-*O*-*β*-D-glucopyranosyl isomer
B15	22.77	$C_{22}H_{21}O_{11}$	461.1078	461.1062	–3.48	299 (100), 446 (75), 225 (42), 207 (20), 425 (20)	chrysoeriol-7-*O*-*β*-D-glucopyranosyl isomer
B16	21.19	$C_{28}H_{31}O_{16}$	623.1607	623.1590	–2.67	315(100), 300(18), 271(5), 255(3), 314(3)	isorhamnetin-3-*O*-*β*-D-rutinoside
B17	20.95	$C_{27}H_{29}O_{14}$	577.1551	577.1527	–4.28	269 (100), 531 (2), 559 (1)	rhoifolin isomer
B18	21.81	$C_{27}H_{29}O_{14}$	577.1551	577.1525	–4.69	269 (100), 413 (5), 431 (3)	rhoifolin isomer
B19	21.74	$C_{22}H_{21}O_{12}$	477.1027	477.1017	–1.07	314 (100), 315 (30), 357 (20), 285 (7)	isorhamnetin-3-*O*-*β*-D-glucopyranoside
C1	10.71	$C_{17}H_{23}O_{11}$	403.1235	403.1277	–2.07	357 (100), 195 (55), 179 (39), 125 (24), 161 (7)	secologanin isomer
C2[#]	14.35	$C_{17}H_{23}O_{11}$	403.1235	403.1233	–0.57	371 (100), 223 (39), 179 (26), 121 (5), 333 (5)	secologanin
C3	4.27	$C_{17}H_{23}O_{10}$	387.1286	387.1276	–2.54	225 (100), 343 (31), 355 (23), 181 (17), 197 (18)	7-*epi*-vogeloside isomer
C4	13.77	$C_{17}H_{23}O_{10}$	387.1286	387.1275	–2.69	225 (100), 355 (28), 181 (21), 343 (17)	7-*epi*-vogeloside isomer
C5	14.55	$C_{17}H_{23}O_{10}$	387.1286	387.1281	–1.27	225 (100), 355 (27), 343 (23), 181 (22)	7-*epi*-vogeloside isomer
C6	2.99	$C_{16}H_{21}O_{11}$	389.1078	389.1066	–3.25	165 (100), 209 (97), 227 (72), 345 (72), 139 (69)	secologanoside isomer
C7	3.82	$C_{16}H_{21}O_{11}$	389.1078	389.1071	–1.99	227 (100), 183 (92), 165 (51), 121 (25), 209 (15)	secologanoside isomer
C8[#]	7.29	$C_{16}H_{21}O_{11}$	389.1078	389.1062	–4.13	345 (100), 209 (21), 121 (14), 165 (13)	secologanoside
C9	7.57	$C_{16}H_{21}O_9$	357.1180	357.1186	–0.55	195 (100), 237 (2), 313 (1)	sweroside isomer
C10[#]	10.67	$C_{16}H_{21}O_9$	357.1180	357.1178	–0.17	195 (100), 237 (8), 313 (2)	sweroside
C11	10.76	$C_{16}H_{21}O_9$	357.1180	357.1177	–0.29	195 (100), 237 (5), 313 (3)	sweroside isomer
C12	4.19	$C_{16}H_{23}O_{10}$	375.1286	375.1281	–1.23	213 (100), 125 (30), 169 (9), 151 (8), 315 (5)	loganin acid isomer
C13	4.84	$C_{16}H_{23}O_{10}$	375.1286	375.1279	–1.17	213 (100), 169 (63), 151 (19), 125 (5)	loganin acid
C14	5.84	$C_{16}H_{23}O_{10}$	375.1286	375.1273	–3.34	213 (100), 169 (17), 151 (4)	loganin acid isomer
C15	6.62	$C_{16}H_{23}O_{10}$	375.1286	375.1278	–2.03	195 (100), 151 (79), 121 (23)	loganin acid isomer
C16	6.62	$C_{17}H_{25}O_{11}$	405.1391	405.1393	0.27	243 (100), 373 (87), 225 (34), 285 (26), 387 (7),	7α-morroniside isomer
C17	7.22	$C_{17}H_{25}O_{11}$	405.1391	405.1398	–0.61	373 (100), 225 (31), 387 (11), 193 (10)	7α-morroniside isomer
C18	13.70	$C_{17}H_{25}O_{11}$	405.1391	405.1389	–0.46	373 (100), 179 (68), 211 (36), 225 (33), 387 (10)	7α-morroniside isomer
C19	14.48	$C_{17}H_{25}O_{11}$	405.1391	405.1388	–0.93	373 (100), 225 (17), 371 (9), 179 (8), 387 (2)	7α-morroniside isomer
C20	2.14	$C_{16}H_{21}O_{10}$	373.1129	373.1119	–1.01	193 (100), 149 (28), 167 (7), 179 (4)	swertiamarin isomer
C21	7.89	$C_{16}H_{21}H_{10}$	373.1129	373.1128	–0.16	193 (100), 149 (27), 167 (7), 179 (3), 123 (3)	swertiamarin
C22	5.30	$C_{16}H_{21}H_{10}$	373.1129	373.1128	–0.16	211 (100), 167 (38), 149 (16), 123 (12), 193 (11)	secologanic acid
C23	22.45	$C_{34}H_{45}O_{19}$	757.2549	757.2529	–2.02	595 (100), 525 (93), 493 (49), 577 (20)	centauroside isomer
C24	23.67	$C_{34}H_{45}O_{19}$	757.2549	757.2526	–2.26	595 (100), 525 (53), 493 (34), 577 (11)	centauroside isomer

Continued

Peak	t_R/min	Formula $[M-H]^-$	Theoretical mass *m/z*	Experimental mass *m/z*	Error (ppm)	MS/MS Fragment ions	Identification/Reactions
C25	4.20	$C_{17}H_{25}O_{12}$	421.1340	421.1339	–0.48	241 (100), 375 (99), 165 (44), 377 (24), 331 (18), 403 (16), 259 (15)	alpigenoside isomer
C26	4.57	$C_{17}H_{25}O_{12}$	421.1340	421.1347	1.53	241 (100), 389 (18), 139 (12), 127 (6), 179 (5), 165 (6), 259 (2)	alpigenoside isomer
C27	4.81	$C_{17}H_{25}O_{12}$	421.1340	421.1335	–1.21	241 (100), 389 (21), 139 (12), 179 (8), 127 (8), 259 (4)	alpigenoside isomer
C28	5.84	$C_{17}H_{25}O_{12}$	421.1340	421.1338	–0.55	241 (100), 389 (17), 139 (11), 179 (8), 377 (11), 127 (6), 259 (2)	alpigenoside isomer
C29	16.33	$C_{18}H_{25}O_{11}$	417.1391	417.1390	–0.06	341 (100), 237 (10), 179 (9), 255 (6)	dimethyl-secologanoside
D1*	3.15	$C_{16}H_{21}O_{12}S$	437.0748	437.0720	–1.52	193 (100), 149 (46), 373 (19), 355 (5)	secologanic acid + SO_2
D2*	1.93	$C_{16}H_{23}O_{13}S$	455.0854	455.0836	–0.69	373 (100), 411 (32), 437 (29), 193 (17), 211 (8)	secologanic acid sulfite esterification
D3*	2.15	$C_{16}H_{23}O_{13}S$	455.0854	455.0822	–0.80	373 (100), 437 (62), 411 (37), 193 (22), 211 (19)	secologanic acid sulfite esterification
D4*	1.81	$C_{16}H_{23}O_{11}$	391.1234	391.1231	–1.62	229 (100), 211 (39), 193 (20), 185 (17), 167 (10), 149 (8)	secologanic acid + H/H_2Odification
D5*	2.45	$C_{16}H_{23}O_{11}$	391.1234	391.1255	–0.80	211 (100), 229 (27), 193 (15), 167 (10), 149 (8), 185 (2)	secologanic acid + H/H_2Oacidification
D6*	1.63	$C_{16}H_{17}O_{12}S$	433.0435	433.0429	–1.34	241 (100), 415 (25), 353 (21), 161 (7), 191 (7), 287 (7)	CQA sulfation
D7*	2.53	$C_{16}H_{17}O_{12}S$	433.0435	433.0427	–1.99	415 (100), 387 (32), 353 (21), 241 (18), 353 (13)	CQA sulfation
D8*	2.66	$C_{16}H_{17}O_{12}S$	433.0435	433.0433	–0.44	241 (100), 415 (24), 387 (19), 259 (11), 353 (10)	CQA sulfation
D9*	4.62	$C_{16}H_{17}O_{12}S$	433.0435	433.0430	–1.14	415 (100), 387 (15), 259 (10)	CQA sulfation
D10*	5.01	$C_{16}H_{17}O_{12}S$	433.0435	433.0424	–2.74	415 (100), 241 (23), 161 (12), 259 (8), 387 (3)	CQA sulfation
D11*	1.12	$C_{16}H_{19}O_{12}S$	435.0591	435.0574	–1.74	353 (100), 191 (12), 179 (5)	CQA sulfite esterification
D12*	16.70	$C_{25}H_{23}O_{15}S$	595.0752	595.0750	–0.44	549 (100), 577 (91), 415 (9), 241 (5), 259 (4)	DiCQA sulfation
D13*	16.98	$C_{25}H_{23}O_{15}S$	595.0752	595.0748	–0.65	549 (100), 577 (77), 415 (7), 301 (4), 397 (2)	DiCQA sulfation
D14*	17.61	$C_{25}H_{23}O_{15}S$	595.0752	595.0737	–2.49	577 (100), 549 (22), 415 (18), 433 (15), 241 (4), 259 (4)	DiCQA sulfation
D15*	17.89	$C_{25}H_{23}O_{15}S$	595.0752	595.0745	–1.27	577 (100), 549 (21), 415 (8), 433 (5), 259 (2)	DiCQA sulfation
D16*	19.38	$C_{25}H_{23}O_{15}S$	595.0752	595.0745	–1.27	577 (100), 549 (77), 415 (11), 433 (6), 397 (3)	DiCQA sulfation
D17*	8.73	$C_{21}H_{19}O_{15}S$	543.0439	543.0431	–1.41	463 (100), 381 (75), 453 (35), 423 (32), 525 (18), 301 (14)	hyperoside sulfation
D18*	12.76	$C_{21}H_{19}O_{15}S$	543.0439	543.0432	–1.30	381 (100), 301 (18), 381 (9), 463 (1)	hyperoside sulfation
D19*	17.34	$C_{21}H_{19}O_{14}S$	527.0490	527.0494	0.83	447 (100), 285 (7), 481 (3)	luteolin-7-*O*-glucoside sulfation

A: chlorogenic acids; B: flavonoids; C: iridoid; D*: newly-generated compounds[#]: Unambiguously identification

$[M - H]^-$ ions of CGAs could easily eliminate cinnamic acid moiety, quinic acid moiety and H_2O to afford their respective DPIs, which could provide supplementary information for the structural identification of CGAs. In brief, there were fourteen kinds of identified CGAs including three CQAs, three *p*CoQAs, three FQAs, two SQAs, three DiCQAs, six CQA glycosides, three CFQAs, five FQA glycosides, two DiCQA glycosides, two cinnamic acids, three PCAs, two caffeic acids, eight *p*CoCQAs and one TriCQA from the SF-LJF extract.

Compounds **A4**−**A6** produced $[M - H]^-$ ions at *m/z* 353.0864, 353.0865 and 353.0872 ($C_{16}H_{17}O_9$, mass error within ± 5 ppm), orderly. In the ESI-MS/MS spectra, they all generated the significant ESI-MS^2 DPIs at *m/z* 191 [quinic acid − H]$^-$, 179 [caffiec acid − H]$^-$ and 173 [quinic acid − H − H_2O]$^-$, which could be adopted to confirm compounds **A4**−**A6** as CQAs. According to the previous reports, the relative intensities of ESI-MS^2 base peak ion and dominant product ions could ascertain the linkage position of caffeoyl group on quinic acid [17-18]. When the caffeoyl group was linked at 4-OH position, *m/z* 173 would be the ESI-MS^2 base peak. When caffeoyl group was linked to quinic acid at 3-OH or 5-OH position, *m/z* 191 would be the ESI-MS^2 base peak ion, and *m/z* 179 was much more important for 3-CQA than 5-CQA. Therefore, compounds **A4**−**A6** were respectively identified as 3-CQA, 5-CQA and 4-CQA, which were all confirmed by comparison with the corresponding reference standards.

Compounds **A20**−**A22** possessed their respective $[M - H]^-$ ions at *m/z* 515.1176, 515.1177 and 515.1180 ($C_{25}H_{23}O_{11}$, mass error within ± 5 ppm). They all generated $[M - H - caffeoyl]^-$ ion at *m/z* 353 in their ESI-MS^2 spectra. However, their ESI-MS^3 spectra were significantly different. **A21** yielded its ESI-MS^3 base peak ion at *m/z* 191 and secondary peak ion at *m/z* 179 (> 40%), indicating it could be attributed to 3-substituted quinic acid. By comparison with the reference substance, **A21** were interpreted as 3, 5-DiCQA. The other product ion just like $[M - H - Caffeoyl - H_2O]^-$ ion at *m/z* 173 was also observed. Therefore, combined with reference comparison, fragmentation pathway analysis and bibliography data [19-20], **A22** was unambiguously assigned as 4, 5-DiCQA, while **A20** was tentatively determined as 3, 4-DiCQA (Fig. 4).

Compounds **A23**-**A28** possessed $[M - H]^-$ ions at *m/z* 515.1387, 515.1392 and 515.1391 ($C_{22}H_{27}O_{14}$, mass error within ± 5 ppm), respectively. The HRMS data showed that their $[M - H]^-$ ions could be reduced by 162 Da owing to CID cracking to afford $[M - H - caffeoyl/Glu]^-$ ion at *m/z* 353, $[M - H - caffeoyl/Glu - H_2O]^-$ ion at *m/z* 335, [quinic acid − H]$^-$ ion at *m/z* 191, and so on. Therefore, compounds **A23**−**A28** were inferred to be monocaffeyl quinic acid glycosides (CQA glycosides). Likewise, compounds **A37**−**A38** which gave $[M - H]^-$ ions at *m/z* 677.1716 ($C_{31}H_{33}O_{17}$, mass error within ± 5 ppm) and similar mass fragmentation pathways could be deduced as DiCQA glycosides. Meanwhile, compound **A39** generated its $[M - H]^-$ ion at *m/z* 677.1501 ($C_{34}H_{29}O_{15}$, mass error within ± 5 ppm). After the collision induced dissociation (CID) cleavage, fragment ions like *m/z* 515 $[M - H - caffeoyl]^-$ and 353 $[M - H - 2caffeoyl]^-$ could be observed in the ESI-MS^2 spectrum indicating the neutral loss of caffeoyl moiety. According to the proposed fragmentation patterns, compound **A39** could be inferred as TriCQA.

Compounds **A40**−**A41** possessed their respective $[M - H]^-$ ions at *m/z* 179.0344 and 179.0435 ($C_9H_7O_4$, mass error within ± 5 ppm). Both compounds yielded $[M - H - CO_2]^-$ ion at *m/z* 135 and $[M - H - H_2O]^-$ ion at *m/z* 161, which were consistent with caffeic acid or its isomers. Therefore, by comparison with the standard substance, compound **A41** was accurately interpreted as caffeic acid, while **A40** was tentatively deduced as caffeic acid isomer.

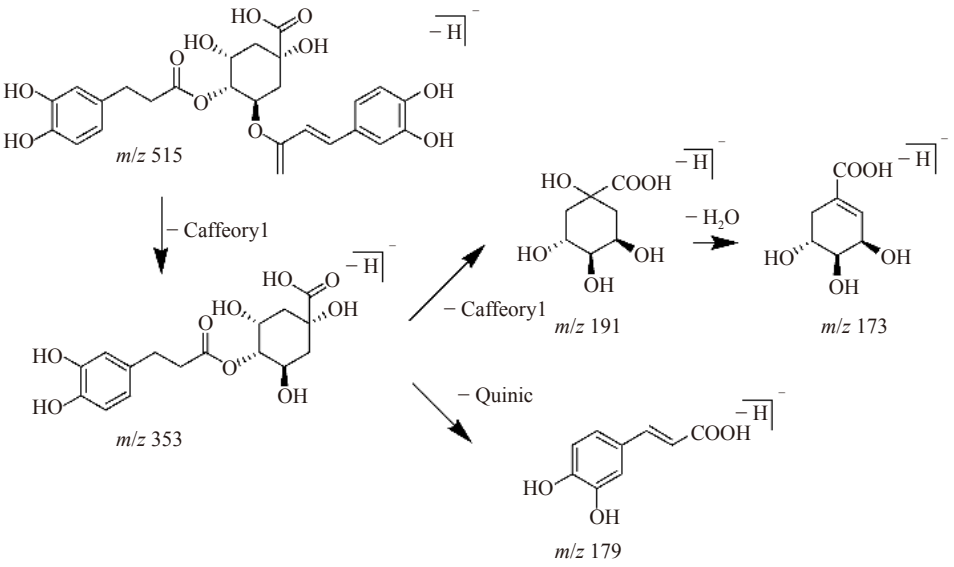

Fig. 4 The proposed fragmentation pathways of 3, 4-DiCQA

Structural identification of flavonoids in SF-LJF extract

Flavonoids glycosides are one important category of components existing in LJF. During the CID-MS/MS experiment, flavonoid glycosides usually first split up the glycosidic bond and then produce aglycone ions. Subsequently, the aglycone ions would be cleaved to form a series of fragment ion peaks [21]. Dehydration, successive losses of CO owing to the presence of a ketone group and phenolic hydroxyl groups, Retro Diels-Alder (RDA) fragmentation, C-ring fragmentation and loss of CHO· are the most possible fragmentation pathways [22]. For example, tricin-7-O-*β*-D-glucopyranoside generated [M − Glu]$^-$ ion at *m/z* 329 and [M − H − Glu]$^-$ ion at *m/z* 328 in its CID-MS/MS fragment cleavage. Meanwhile, rhoifolin further respectively generated [M − H − Rha − Glu]$^-$, [M − H − CH_2OH]$^-$ and [M − H − Glu]$^-$ ion at *m/z* 269, 531 and 431 upon CID mode. Finally, the structures of 19 flavonoids in the SF-LJF extract were characterized.

The compounds **B1**−**B2** generated the respective [M − H]$^-$ ions at *m/z* 447.0900 and 447.0901 ($C_{21}H_{19}O_{11}$, mass error within ± 5 ppm). They yielded a fragment [M − H − Glu]$^-$ ion at *m/z* 285 through losing one molecule of glucose in the ESI-MS^2 spectrum, which were consistent with luteolin-7-*O*-glucoside. Therefore, according to the previous report and reference, compound **B1** was assigned as luteolin-7-*O*-glucoside and **B2** was inferred to be its isomer.

Compounds **B3**−**B5** possessed the identical [M − H]$^-$ ions at *m/z* 593.1472, 593.1467 and 593.1471 ($C_{27}H_{29}O_{15}$, mass error within ± 5 ppm). Upon CID mode, they further generated [M − H − Rha − Glu]$^-$ at *m/z* 285 and [M − H − Rha]$^-$ ion at *m/z* 447, respectively. The appearance of [M − H − 308]$^-$ ion was corresponding to the neutral loss of one rutinose unit. Compared with the reference standard, **B5** was positively deduced to be lonicerin. Meanwhile, combined with bibliography data and fragmentation pathways, the other two compounds **B3**−**B4** were tentatively ascertained as lonicerin isomers.

The compound **B6** generated [M − H]$^-$ ion at *m/z* 491.1170 ($C_{23}H_{23}O_{12}$, mass error within ± 5 ppm). In the MS^2 spectrum, it produced [M − H − CH_3]$^-$ at *m/z* 476, [M − Glu]$^-$ ion at *m/z* 329 and [M − H − Glu]$^-$ ion at *m/z* 328. Compared with the standard substance, compound **B6** was accurately deduced as a tricin- 7-O-*β*-D-glucopyranoside.

Compounds **B7**−**B8** yielded [M − H]$^-$ ions at *m/z* 463.0842 and 463.0841 ($C_{21}H_{19}O_{12}$, mass error within ± 5 ppm). They further generated [M − H − Glu]$^-$ at *m/z* 301 and [M − 2H − Glu]$^-$ ion at *m/z* 300, respectively. By comparison with the standard substance, compound **B8** was positively characterized as hyperoside, and **B7** was inferred to be hyperoside isomer.

Compounds **B9**−**B11** possessed [M − H]$^-$ ions at *m/z* 609.1436, 609.1429 and 609.1408 ($C_{27}H_{29}O_{16}$, mass error within ± 5 ppm). They all generated [M − H − Rha − Glu]$^-$ ion at *m/z* 301 with a high intensity and [M − 2H − Rha − Glu]$^-$ ion at *m/z* 300 in the MS^2 spectrum. Compound **B11** was accurately identified as rutin by comparison with the corresponding reference standard. In addition, according to the fragmentation pathways from the literature data [23], compounds **B9**−**B10** were tentatively assigned to be rutin isomers.

Compounds **B17**−**B18** yielded [M − H]$^-$ ions at *m/z* 577.1527 and 577.1525 ($C_{27}H_{29}O_{14}$, mass error within ± 5 ppm). Upon CID mode, they further generated [M − H − Rha − Glu]$^-$, [M − H − CH_2OH]$^-$ and [M − H − Glu]$^-$ ion at *m/z* 269, 531 and 431, respectively. And thus, compounds **B17**−**B18** were deduced to be quercetin or isomeric quercetin.

Compound **B19** gave [M − H]$^-$ ion at *m/z* 477.1017 ($C_{23}H_{23}O_{12}$, mass error within ± 5 ppm). After the CID cleavage, its further fragmentation resulted in [[M − H − Glu]$^-$ ion at *m/z* 315 and [M − H − Glu − CH_3]$^-$ ion at *m/z* 300, which were consistent with the characteristic fragmentation pathways of flavonoid glycosides. Based on this, compound **B19** was plausibly characterized as isorhamnetin-3-*O*-rutinoside.

Structural identification of iridoid glycosides in SF-LJF extract

In this experiment, a total of 29 constituents attributed to iridoid glycosides were screened and identified from SF-LJF sample according to their retention times, ESI-MS and ESI-MS/MS data. Iridoid glycosides generally contain a glucose moiety attached to C-1 position in their pyran ring. The mass spectrometry cleavage of iridoid glycosides usually lose glucose (162 Da), H_2O (18 Da), CO_2 (44 Da) and CO (28 Da), *etc*. In addition, methoxyl-containing iridoid glycosides ordinarily lose CH_3OH (32 Da). According to the literature data, most of iridoid glycosides gave [M − H]$^-$ ions as the base peak ions in their ESI-MS spectra [24-26].

Compounds **C1**−**C2** possessed predominant [M − H]$^-$ ions at *m/z* 403.1277 and 403.1233 ($C_{17}H_{23}O_{11}$, mass error within ± 5 ppm). In the ESI-MS^2 spectrum, C1 yielded characteristic fragment ion at *m/z* 125 originating from RDA cleavage while [M − H − Glu]$^-$ ion at *m/z* 195 through successive loss of one glucose. In addition, C2 further yielded [M − H − H_2O − CO]$^-$ ion at *m/z* 371, [M − H − Glu − H_2O]$^-$ ion at *m/z* 223 and [M − H − Glu − H_2O − CO_2]$^-$ ion at *m/z* 179, which were consistent with the characteristic fragmentation pathways of secoxyloganin. Therefore, **C2** was tentatively ascertained as secoxyloganin, while **C1** was tentatively presumed to be secoxyloganin isomer.

Compounds **C6**−**C8** gave rise to their respective [M − H]$^-$ ions at *m/z* 389.1066, 389.1071 and 389.1062 ($C_{16}H_{21}O_{11}$, mass error within ± 5 ppm). In their ESI-MS^2 spectra, **C6**−**C8** produced [M − H − CO_2]$^-$ ion at *m/z* 345, [M − H − Glu − H_2O]$^-$ ion at *m/z* 209, [M − H − Glu − CO_2]$^-$ ion at *m/z* 165 and [M − H − Glu]$^-$ ion at *m/z* 227. Further neutral losses of H_2O and CO generated [M − H − Glu − H_2O − CO_2 − CO]$^-$ ion at *m/z* 121. According to the fragmentation cleavage pathways and related literature [27], compounds **C6**−**C7** were characterized to be loganin isomers. After comparing with the reference standard, compound **C8** was accur-

ately judged as secologanin.

Compounds **C9**−**C11** yielded $[M - H]^-$ ions at *m/z* 357.1186, 357.1178 and 357.1177 ($C_{16}H_{21}O_9$, mass error within ± 5 ppm). They all possessed $[M - H - Glu]^-$ ion at *m/z* 195 and $[M - H - CO_2]^-$ ion at *m/z* 313 through losing glucose and CO_2 in their ESI-MS^2 spectra. Combined with standard comparison, **C10** was accurately deduced as sweroside, while **C9** and **C11** were characterized to be sweroside isomers.

Compounds **C12**−**C15** gave their respective $[M - H]^-$ ions at *m/z* 375.1281, 375.1279, 375.1273 and 375.1278 ($C_{16}H_{23}O_{10}$, mass error within ± 5 ppm). Upon CID mode, they further generated $[M - H - Glu]^-$ ion at *m/z* 213, $[M - H - Glu - CO_2]^-$ ion at *m/z* 169 and $[M - H - Glu - CO_2 - H_2O]^-$ ion at *m/z* 151. However, **C15** appeared to be different from the other two compounds might due to its characteristic $[M - H - Glu - H_2O]^-$ ion at *m/z* 195. Finally, compound **C13** was accurately judged as loganic acid. Compounds **C12**, **C14** and **C15** were characterized to be the isomers of loganic acid.

Compounds **C20**−**C22** gave $[M - H]^-$ ions at *m/z* 373.1119, 373.1128 and 373.1118 ($C_{16}H_{21}O_{10}$, mass error within ± 5 ppm) as their respective base peak ion. In the ESI-MS^2 spectrum, **C20** fragmentation pathways were quite similar to those of **C21** producing $[M - H - Glu - H_2O]^-$ ion at *m/z* 193, $[M - H - Glu - H_2O - CO_2]^-$ ion at *m/z* 149 and $[M - H - Glu - CO_2]^-$ ion at *m/z* 167 through losing one molecule of glucose, H_2O and CO_2, orderly. In addition, compound **C22** yielded $[M - H - Glu]^-$ ion at *m/z* 211, $[M - H - Glu - CO_2]^-$ ion at *m/z* 169 and $[M - H - Glu - CO_2 - H_2O]^-$ ion at *m/z* 151, respectively. And then, **C21** and **C20** were respectively deduced to be swertiamarin and its isomer, while **C22** was deduced to be secologanic acid.

Structural identification of newly-generated compounds in SF-LJF extract

In this study, an UHPLC-LTQ-Orbitrap-based method was successfully developed for the structural identification of sulfur-containing constituents in the SF-LJF extract. The resolving power, accurate mass-measurement capability and full spectral sensitivity were fully reflected in this study. As a result, 19 newly-generated compounds (including 17 sulfur-containing derivatives) were finally identified according to the chromatographic behavior, ESI-MS and ESI-MS/MS data and literature reports (Fig. 5). Some original compounds existing in NSF-LJF could generally lead to the reactions such as sulfation esterification or sulfitation esterification during the sulfur fumigation process. These new-generated compounds further yielded the characteristic fragment ions including $[M - H - SO_2]^-$, $[M - H - H_2SO_3]^-$ and $[M - H - SO_3]^-$ in their ESI-MS^2 spectra.

Secologanic acid is one of the main iridoid terpenoids contained in LJF with hemiacetal hydroxyl group in their molecular structures. Sulfur fumigation could reduce the content of secologanic acid and then produced sulfite derivatives B-E [26, 28]. The possible chemical transformation mechanisms were illustrated in Fig. 6.

Compound **D1** gave rise to $[M - H]^-$ ion at *m/z* 437.0720 ($C_{16}H_{21}O_{12}S$, mass error within ± 5 ppm). It further yielded $[M - H - SO_2 - Glu - H_2O]^-$ ion at *m/z* 193 and $[M - H - SO_2 - Glu - H_2O - CO_2]^-$ ion at *m/z* 149 through successive loss of glucose, H_2O or CO_2. The characteristic fragment ion at *m/z* 373 $[M - H - SO_2]^-$ with the highest abundance in the ESI-MS^2 spectrum indicated that sulfur dioxide should be introduced into secologanic acid. Therefore, compound **D1** was tentatively presumed to be the sulfate esterification product of secologanic acid.

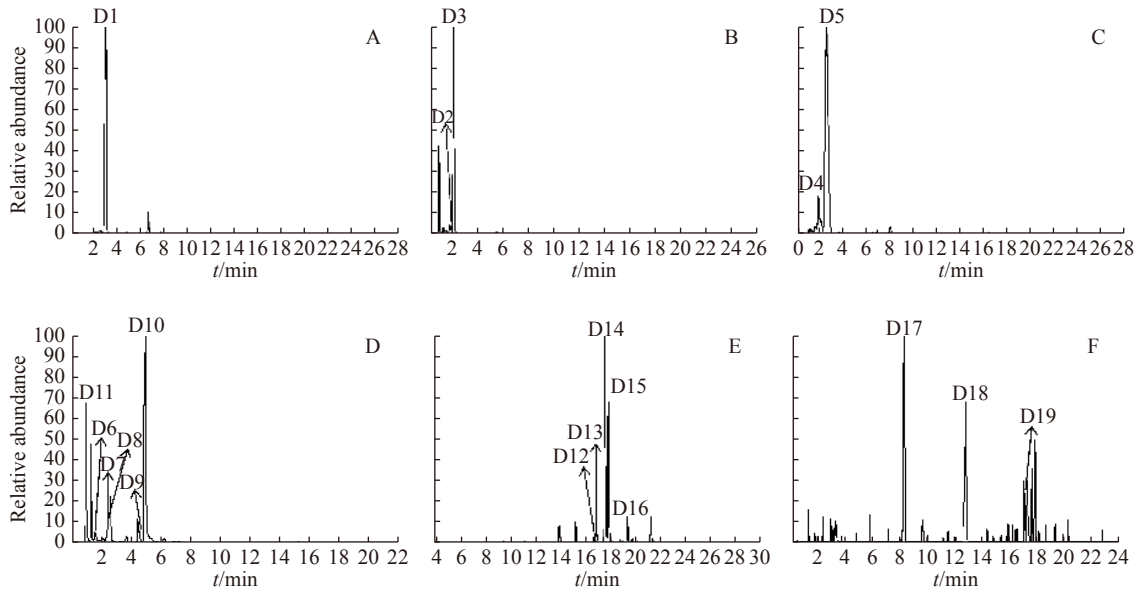

Fig. 5 HREIC chromatograms of sulfur-containing compounds (mass error within ± 5 ppm): (A) *m/z* 437.0748; (B) *m/z* 455.0854; (C) *m/z* 391.1234; (D) *m/z* 433.0435, 435.0591; (E) *m/z* 595.0762; (F) *m/z* 543.0439, 527.0490

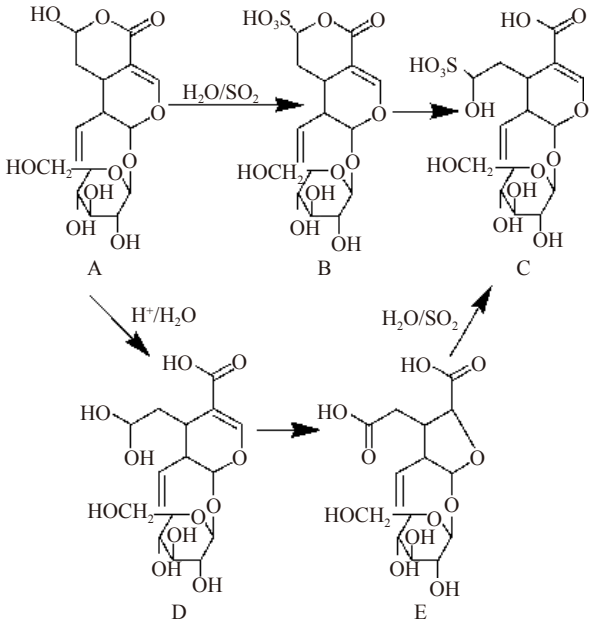

Fig. 6 Chemical transformation mechanism of sulfite fumigation of secologanic acid

Compounds **D2**−**D3** yielded $[M - H]^-$ ions at *m/z* 455.0836 and 455.0822 ($C_{16}H_{23}O_{13}S$, mass error within ± 5 ppm). In their ESI-MS^2 spectra, the ESI-MS/MS fragmentation pathways of **D2** were also quite similar to those of **D3**, since both of their further fragmentations resulted in $[M - H - H_2SO_3]^-$ ion at *m/z* 373, $[M - H - H_2O]^-$ ion at *m/z* 437, $[M - H - CO_2]^-$ ion at *m/z* 411, $[M - H - H_2SO_3 - Glu - H_2O]^-$ ion at *m/z* 193 and $[M - H - H_2SO_3 - Glu]^-$ ion at *m/z* 211. The distinctive fragment ion at *m/z* 373 $[M - H - H_2SO_3]^-$ due to the introduction of sulfite esterification could confirm **D2** and **D3** to be sulfite esterification products of secologanic acid.

Compounds **D4** and **D5** possessed their respective $[M - H]^-$ ions at *m/z* 391.1231 and 391.1255 ($C_{16}H_{23}O_{11}$, mass error within ± 5 ppm). They possessed the similar fragmentation pathways in ESI-MS^2 spectra as for the produced $[M - H - Glu]^-$ ion at *m/z* 229, $[M - H - Glu - H_2O]^-$ ion at *m/z* 211, $[M - H - Glu - 2H_2O]^-$ ion at *m/z* 193, $[M - H - Glu - H_2O - CO_2]^-$ ion at *m/z* 167 and $[M - H - Glu - 2H_2O - CO_2]^-$ ion at *m/z* 149, respectively. Therefore, compounds **D4** and **D5** were interpreted to be acidified products of secologanic acid.

Compounds **D6**−**D10** yielded $[M - H]^-$ ions at *m/z* 433.0429, 433.0427, 433.0433 and 433.0430 ($C_{16}H_{17}O_{12}S$, mass error within ± 5 ppm), respectively. Their further fragmentation resulted in $[M - H - SO_3]^-$ ion at *m/z* 353, [caffeic acid − H + SO_3]$^-$ ion at *m/z* 259, [caffeic acid − H + SO_3 − H_2O]$^-$ ion at *m/z* 241, $[M - H - H_2O]^-$ ion at *m/z* 415 and $[M - H - H_2O - CO]^-$ ion at *m/z* 387 in their ESI-MS^2 spectra. Moreover, the characteristic fragment ions at *m/z* 353, 259 and 241 suggested the occurrence of sulfate esterification reaction. And thus, compounds **D6**−**D10** were all inferred to the sulfated products of CQA. Meanwhile, compound **D11** yielded $[M - H]^-$ ion at *m/z* 435.0574 ($C_{16}H_{19}O_{12}S$, mass error within ± 5 ppm). It also further afforded the distinctive $[M - H_2SO_3]^-$ ion at *m/z* 353. Therefore, compound **D11** were identified to be the sulfite esterification product of CQA.

Compounds **D12**−**D16** generated their respective $[M - H]^-$ ions at *m/z* 595.0750, 595.0748, 595.0737, 595.0745 and 595.0745 ($C_{25}H_{23}O_{15}S$, mass error within ± 5 ppm). In their ESI-MS^2 spectra, it generated a serial of fragment ions at *m/z* 577 $[M - H - H_2O]^-$, *m/z* 549 $[M - H - H_2O - CO]^-$, *m/z* 259 [caffeic − H + SO_3]$^-$ and *m/z* 241 [caffeic − H + SO_3 − H_2O]$^-$. The presence of distinctive ions [caffeic − H + SO_3]$^-$ at *m/z* 259 and [caffeic − H + SO_3 − H_2O]$^-$ at *m/z* 241 also suggested that the occurrence of sulfation reaction. According to the fragmentation pathways and reference standard, compounds **D12**−**D16** were tentatively presumed to be DiCQAs sulfation.

Compounds **D17**−**D18** gave pesudomolecular ions $[M - H]^-$ at *m/z* 543.0431 and 543.0432 ($C_{21}H_{19}O_{15}S$, mass error within ± 5 ppm) as the base peak ions. In the ESI-MS^2 spectra, they all further yielded characteristic $[M - H - SO_3]^-$ ion at *m/z* 463, which indicated the sulfation reaction occurred. Finally, compounds **D17**−**D18** were deduced as the sulfated products of hyperoside.

Compound **D19** possessed $[M - H]^-$ ion at *m/z* 527.0490 ($C_{21}H_{19}O_{14}S$, mass error within ± 5 ppm). In its ESI-MS^2 spectrum, the $[M - H - CH_2OH]^-$ ion at *m/z* 447 and $[M - H - SO_3 - Glu]^-$ ion at *m/z* 285 were all formed. In addition, compound **D19** also generated the fragment ion at *m/z* 447 $[M - H - SO_3]^-$, which suggested the occurrence of sulfite reaction. Therefore, **D19** was characterized to be luteolin-7-O-glucoside sulfation.

Meanwhile, 5-CQA, one of the representative chemical constitutes existing in LJF was chosen for the validation of those new-generated sulfur-containing derivatives. Under the premise that it did not influence the result reliability, both SF-5-CQA and 5-CQA were synchronously analyzed using the same method. As a result, the existence of new-generated sulfur-containing derivatives, such as 5-CQA sulfation could be observed (Fig. 7). The structures of these newly emerged peaks were confirmed as the rudimentary sulfur-containing derivatives of 5-CQA, which were 79.95 Da (SO_3) more than that of 5-CQA. Therefore, all the results demonstrated the occurrence of 5-CQA sulfation during the process of sulfur fumigation, which further validated that the SF transformations really occurred to the constituents existing in LJF to some extent.

Conclusions

Sulfur was reported to cause chemical transformation of original bioactive components in TCMs or their extracts leading to the bioactivities, pharmacokinetics and even toxicities consequently [29-32]. Based on this, it is of great significance to study the sulfur-fumigation state of TCMs for the sake of

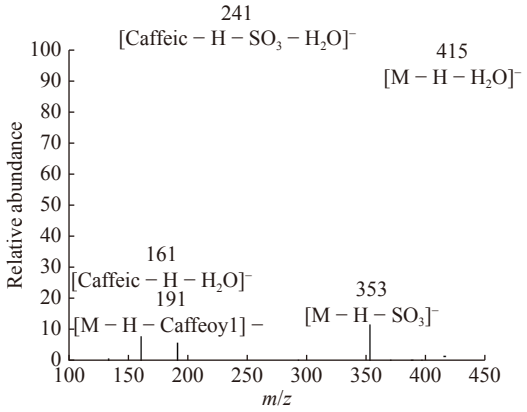

Fig. 7 The ESI-MS^2 spectrum of SF-5-CQA sulfation

controlling quality. It is worth noting that SF-LJF used in this paper was excessive sulfur fumigation in the laboratory, which imitated the operation method in producing area. In addition, UHPLC-LTQ-Orbitrap MS was used to acquire data about SF-LJF, which greatly improved natural products analysis. Combining with the fragmentation rule, chromatographic behavior, diagnostic ions and related literature data, the patterns of fragmentation observed were compared with those of the reference substances. Finally, 113 compounds were identified from SF-LJF. These components included 46 CGAs, 19 flavonoids, 29 iridoid glycosides and 19 newly-generated compounds (including 17 sulfur-containing derivatives). Among them, the new sulfur-containing derivatives compounds were new generated and other most compounds were both discovered in the two kind samples. By comparison with LJF, the components of SF-LJF were having significant changes such as the reduction of iridoid terpenoids and the formation of sulfate esters, which was consistent with the previous reports. In addition, it was discovered that the occurrence of sulfate or sulfite esterification reactions resulting in the emergence of many new sulfur-containing components during SF process. In conclusion, the detailed mass spectrometric fragmentation regularities of various compounds were elaborated and the material basis of SF-LJF was comprehensively characterized, which provided a solid foundation for the quality control of SF-LJF and its related drugs and foods. SF is a considerable problem that can not be neglected in TCMs industry. This paper owing to its abundant information expounds the detailed changes of chemical composition in the process of SF by taking LJF as an example. Then, the secret behind changes has been revealed which relys on using UHPLC-LTQ-Orbitrap MS method under our in-depth study. Moreover, this study sets a good example for the accurate identification of chemical constituents after SF and further provides guidance for quality control of TCMs.

Abbreviations

Lonicerae japonicae Flos: LJF; traditional Chinese medicines: TCMs; ultra-high performance liquid chromatography coupled with linear ion trap-Orbitrap mass spectrometry: UHPLC-LTQ-Orbitrap MS; sulfur-fumigated LJF: SF-LJF; non-sulfur-fumigated LJF: NSF-LJF; diagnostic product ions: DPIs; high-resolution mass spectrometry: UHPLC-HRMS; chlorogenic acids: CGAs; caffeoylquinic acid: CQA; dicaffeoylquinic acid: DiCQA; *p*-coumaroylquinic acid: *p*CoQA; feruloylquinic acid: FQA; sinapoylquinic acid: SQA; caffeoylferuloylquinic acid: CFQA; *p*-coumaroyl-caffeoylquinic acid: *p*CoCQA; tricaffeoylquinic acid: TriCQA; protocatechuic acids: PCA; retention time: t_R; 5-caffeoylquinic acid: 5-CQA; 3-caffeoylquinic acid: 3-CQA; 4-caffeoylquinic acid: 4-CQA; 3,5-dicaffeoylquinic acid: 3,5-CQA; 3,4-dicaffeoylquinic acid: 3,4-CQA; 4,5-dicaffeoylquinic acid: 4,5-CQA; formic acid: FA; dynamic exclusion: DE; Ring Double Bond: RDB; total ion chromatograms: TICs; collision induced dissociation: CID; Retro Diels-Alder: RDA.

References

[1] *Pharmacopeia of the People's Republic of China* [S]. Part 1. Beijing: China Medical Science Press, 2015.

[2] Kang OH, Choi JG, Lee JH, *et al*. Luteolin isolated from the flowers of *Lonicera japonica* suppresses inflammatory mediator release by blocking NF-κB and MAPKs activation pathways in HMC-1 [J]. *Molecules*, 2010, **15**(1): 385–389.

[3] Ning W, Peng X, Ma LY, *et al*. Enhanced secondary metabolites production and antioxidant activity in postharvest *Lonicera japonica* Thunb. in response to UV radiation [J]. *Innov Food Sci Emerg*, 2012, **13**: 231–243.

[4] Tian J, Che HL, Ha D, *et al*. Characterization and anti-allergic effect of a polysaccharide from the flower buds of *Lonicera japonica* [J]. *Carbohyd Polym*, 2012, **90**(4): 1642–1647.

[5] Jeong YT, Jeong SC, Hwang JS, *et al*. Modulation effects of sweroside isolated from the *Lonicera japonica* on melanin synthesis [J]. *Chem-Biol Interact*, 2015, **238**: 33–39.

[6] Wang Z, Clifford MN, Sharp P. Analysis of chlorogenic acids in beverages prepared from Chinese health foods and investigation, *in vitro*, of effects on glucose absorption in cultured Caco-2 cells [J]. *Food Chem*, 2008, **108**(1): 369–373.

[7] Lee EJ, Ju SK, Kim HP, *et al*. Phenolic constituents from the flower buds of *Lonicera japonica* and their 5-lipoxygenase inhibitory activities [J]. *Food Chem*, 2010, **120**(1): 134–139.

[8] Wang CZ, Aung HH, Ni M, *et al*. Red American ginseng: Ginsenoside constituents and antiproliferative activities of heat-processed *Panax quinquefolius* roots [J]. *Planta Med*, 2007, **73**(07): 669–674.

[9] Wang ZJ, Guan X, Wang J, *et al*. Determination of sulphur dioxide in Chinese herbal medicines by iodine titration method [J]. *Chin Tradit Herb Drugs*, 2000, **31**: 97–99.

[10] Wang GY, Tian Y. Differences in properties and flavors of Chinese medicinal materials caused by different processing methods [J]. *J Chin Med Mat*, 1998, **1**: 21–21.

[11] Li SL, Shen H, Zhu LY, *et al*. Ultra-high-performance liquid chromatography-quadrupole/time of flight mass spectrometry based chemical profiling approach to rapidly reveal chemical transformation of sulfur-fumigated medicinal herbs, a case study on white ginseng [J]. *J Chromatogr A*, 2012, **1231**: 31–45.

[12] Wang F, Zhang JY, Yin PH, *et al*. Rapid identification of polyphenols in Kudiezi injection with a practical technique of mass defect filter based on high-performance liquid chromatography coupled with linear ion trap/orbitrap mass spectrometry [J]. *Anal Methods (UK)*, 2014, **6**(10): 3515–3523.

[13] Zhang JY, Li N, Che YY, *et al*. Characterization of seventy

polymethoxylated flavonoids (PMFs) in the leaves of *Murraya paniculata* by on-line high-performance liquid chromatography coupled to photodiode array detection and electrospray tandem mass spectrometry [J]. *J Pharm Biomed*, 2011, **56**(5): 950–961.

[14] Zhang JY, Lu JQ, Wang F, *et al*. A strategy of EIC-MS coupled with diagnostic product ions analysis for efficient discovery of new hydroxylated polymethoxyflavonoid glycosides from the leaves of *Murraya paniculata* L. using HPLC-DAD-MS/MS [J]. *Anal Methods (UK)*, 2013, **5**(11): 2880–2891.

[15] Niranjan A, Mishra S, Lehri A, *et al*. Identification and quantification of heterologous compounds parthenin and organic acids in *Parthenium hysterophorus* L. using HPLC-PDA-MS-MS [J]. *Anal Lett*, 2013, **46**(1): 48–59.

[16] Ma XQ, Leung AKM, Chan CL, *et al*. UHPLC UHD Q-TOF MS/MS analysis of the impact of sulfur fumigation on the chemical profile of Codonopsis Radix (Dangshen) [J]. *Analyst*, 2014, **139**: 505–516.

[17] Clifford MN, Johnston KL, Knight S, *et al*. Hierarchical scheme for LC-MS^n identification of chlorogenic acids [J]. *J Agr Food Chem*, 2003, **51**(10): 900–911.

[18] Möller B, Herrmann K. Quinic acid esters of hydroxycinnamic acids in stone and pome fruit [J]. *Phytochemistry*, 1983, **22**(2): 477–481.

[19] Clifford MN, Kirkpatrick J, Kuhnert N, *et al*. LC-MS^n analysis of the cis isomers of chlorogenic acids [J]. *Food Chem*, 2008, **106**(1): 379–385.

[20] Zhang JY, Wang ZJ, Li Y, *et al*. A strategy for comprehensive identification of sequential constituents using ultra-High-performance liquid chromatography coupled with linear ion trap-Orbitrap mass spectrometer, application study on chlorogenic acids in Flos Lonicerae Japonicae [J]. *Talanta*, 2016, **147**: 16–39.

[21] Cai W. Targeted separation and *in vivo* metabolism of sesquiterpene lactone analogues from Kudiezi [D]. Beijing: Beijing University of Chinese Medicine, 2016.

[22] Qi LW, Chen CY, Li P, *et al*. Structural characterization andidentification of iridoid glycosides, saponins, phenolic acids and flavonoids in Flos Lonicerae Japonicae by a fast liquid chromatography method with diode-array detection and time-of-flight mass spectrometry [J]. *Rapid Commun Mass SP*, 2009, **23**(19): 3227–3242.

[23] Choi CW, Jung HA, Kang SS, *et al*. Antioxidant constitutes and a new triterpenoid glycoside from Flos Lonicerae [J]. *Arch Pharm Res*, 2007, **30**(1): 1–7.

[24] Ren LL, Xue XY, Zhang FF, *et al*. Studies of iridoid glycosides using liquid chromatography/electrospray ionization tandem mass spectrometry [J]. *Rapid Commun Mass SP*, 2007, **21**(18): 3039–3050.

[25] Es-Safi NE, Kerhoas L, Ducrot PH. Fragmentation study of iridoid glucosides through positive and negative electrospray ionization, collision-induced dissociation and tandem mass spectrometry [J]. *Rapid Commun Mass SP*, 2007, **21**(7): 1165–1175.

[26] Guo AL, Chen LM, Wang YM, *et al*. Influence of sulfur fumigation on the chemical constituents and antioxidant activity of buds of *Lonicera japonica* [J]. *Molecules*, 2014, **19**(10): 16640–16655.

[27] Song Y, Li SL, Wu MH, *et al*. Qualitative and quantitative analysis of iridoid glycosides in the flower buds of *Lonicera* species by capillary high performance liquid chromatography coupled with mass spectrometric detector [J]. *Anal Chim Acta*, 2006, **564**(2): 211–218.

[28] Li ZY, Gao HM, Sun J, *et al*. Secoiridoid sulfonates from the sulfiting-processed buds of *Lonicera japonica* [J]. *Helv Chim Acta*, 2012, **95**(7): 1144–1151.

[29] Hayes PYN, Lehmann RP, Penman KG, *et al*. Sodium paeoniflorin sulfonate, a process derived artifact from paeoniflorin [J]. *Tetrahedron Lett*, 2005, **46**(15): 2615–2618.

[30] Li SL, Song JZ, Choi F, *et al*. Chemical profiling of Radix Paeoniae evaluated by ultra-performance liquid chromatography/photo-diode-array/quadrupole time-of-flight mass spectrometry [J]. *J Pharm Biomed*, 2009, **49**(2): 253–266.

[31] Liu L, Zhu XM, Wang QJ, *et al*. Enzymatic preparation of 20(*S*, *R*)-proto panaxadiol by transformation of 20(*S*, *R*)-Rg3 from black ginseng [J]. *Phytochemistry*, 2010, **71**(13): 1514–1520.

[32] Qu CL, Bai YP, Jin XQ, *et al*. Study on ginsenosides in different parts and ages of *Panax quinquefolius* L. [J]. *Food Chem*, 2009, **115**(1): 340–346.

Cite this article as: LIU Zi-Han, WANG Yu-Qi, MEI Xiao-Dan, WANG Fei, YANG Xian-Zhao, LI Xiao-Dong, JIANG Feng, ZHANG Jia-Yu. Comprehensive analysis of the chemical constituents in sulfur-fumigated Lonicerae Japonicae Flos using UH-PLC-LTQ-Orbitrap mass spectrometry [J]. *Chin J Nat Med*, 2020, **18**(2): 148-160.